The Role of Tissue Heterogeneity in Neural Stimulation by Applied Electric Fields

Pedro C. Miranda, Ludovic Correia, Ricardo Salvador, and Peter J. Basser

Abstract— **Heterogeneity of electrical conductivity is a new mechanism by which excitable tissues can be stimulated via applied electric fields. Stimulation of axons crossing internal boundaries can arise at those boundaries where the electric conductivity of the volume conductor changes abruptly. The effectiveness of this and other stimulation mechanisms was compared in the context of transcranial magnetic stimulation. While, for a given stimulation intensity, the largest membrane depolarization occurred where an axon terminates or bends sharply in a high electric field region, a slightly smaller membrane depolarization, still sufficient to generate action potentials, also occurred at an internal boundary simulating a white matter-grey matter interface. Tissue heterogeneity can also give rise to local electric field gradients that are considerably stronger and more focal than those impressed by the stimulation coil. Tissue heterogeneity may play an important role in electric and magnetic "far field" stimulation.**

I. INTRODUCTION

NEURAL stimulation using low frequency electric fields may be achieved through a variety of mechanisms. For long, straight, uniform unmyelinated fibres, the steady state change in membrane potential V' due to a subthreshold stimulus is given by [1, 2]

$$V'(x) = -\lambda^2 \frac{\partial E_x(x)}{\partial x},\qquad(1)$$

where E_x is the component of the total electric field in the direction of the axon, λ is the membrane space constant, and assuming that $V'(x)$ varies slowly with x. The term on the right is usually referred to as the activation function.

In general, however, axons may terminate, follow curved paths, branch, or change diameter. In these cases, membrane polarization can take place even in the absence of an electric field gradient [3, 4]. For a straight semi-infinite ($x \geq 0$) fiber in a uniform electric field, a significant steady state change in membrane potential occurs only in the vicinity of the

termination (at $x = 0$), given by

$$V'(x) = -\lambda\, E_x(x) e^{-\frac{x}{\lambda}}.\qquad(2)$$

In this study we investigate the possibility that tissue heterogeneity may also affect significantly the transmembrane potential of excitable cells, even when they are subjected to an applied electric field whose amplitude may be uniform on the scale of the membrane length constant. Indeed, tissue heterogeneity can introduce large local changes in the spatial distribution of both the electric field and the electric field gradient, due to charge accumulating at the boundaries separating tissues with different electrical conductivities [5-9].

We also consider, for the first time, the effect of tissue heterogeneity on the membrane potential of an axon that crosses an internal boundary, such as a white matter-grey matter interface. The accumulation of charge at the boundary gives rise to a discontinuity ΔE_n in the normal component of the electric field, whose magnitude is given by

$$\Delta E_n = 2\left(\frac{\sigma_1 - \sigma_2}{\sigma_1 + \sigma_2}\right) \vec{E} \cdot \vec{n}\qquad(3)$$

where $\vec{E}$ is the total electric field at the boundary and σ_1 is the electric conductivity of the tissue anterior to the interface, as determined by the direction of the electric field [9]. If the jump in the normal component of the electric field is modelled as a Heaviside step function of height ΔE_n then the derivative of the electric field along the direction of the axon (x) is a Dirac delta function, $\Delta E_x\,\delta(x)$, and the steady-state solution for the cable equation is

$$V'(x) = -\frac{\lambda\,\Delta E_x}{2} e^{-\frac{|x|}{\lambda}}\qquad(4)$$

where $\Delta E_x = \Delta E_n \cos(\theta)$, θ being the angle between the normal and the axon's axis.

Here, we examine the relative importance of the above-mentioned neural stimulation mechanisms by comparing the magnitude of the changes in membrane potential due to the electric field, λE_x, to the electric field gradient, $\lambda^2 \frac{\partial E_x}{\partial x}$,

and to the electric field discontinuity, $\lambda \Delta E_x/2$, in different situations. In all cases the electric field is induced by a magnetic stimulator with a figure-of-8 coil.

II. METHODS

Some knowledge of the axonal length constant, λ, is required to compare the changes in membrane potential caused by the different stimulation mechanisms. We have assumed an axon diameter of 10 μm and taken $\lambda = 2$ mm in our calculations.

The coil used in these calculations replicates Magstim's 70 mm double coil, as described in [10]. The rate of change of the current was set to 67 A/μs in the first two calculations and to 61.2 A/μs in the last calculation.

A spherical head model with a radius of 92 mm was used in the first two calculations. The sphere is centered on the origin of the coordinate system and the coil is positioned in the plane z = 102 mm, tangential to the sphere. The line passing through the centre of both wings is aligned parallel to the x-axis; under the centre of the coil the induced electric field points along the y-axis.

For the homogeneous spherical head model the total induced electric field was calculated using Eaton's formulae [11]. The cartesian components of the electric field were computed on a grid of 11x11 points lying on a spherical surface of radius 77 mm, which corresponds approximately to 3 mm below the cortical surface [6]. The components of the electric field gradient tensor were estimated at a given point in the grid by computing the electric field components at six neighboring points displaced by ±1 mm along each axis. For a given direction specified by a vector $\vec{n}$, the net electric field gradient along that direction is given by $\vec{n}^T (\nabla \vec{E})\,\vec{n}$. We will refer to this scalar quantity as the directional derivative of the electric field.

For the heterogeneous spherical head model, a cylindrical inclusion was placed below the coil centre with its axis parallel to the y-axis, in the plane z = 72 mm. The length of the cylinder extended from y = -5 mm to y = +5 mm, with a radius of 5 mm. The electric conductivities of the sphere and the cylinder were taken to be 0.333 S/m (gray matter [12]) and 1.79 S/m (cerebrospinal fluid [13]), respectively. In this configuration (see inset in fig. 2) and near the centre of the cylinder bases, only the component of the electric field parallel to the cylinder axis, E_y, is significantly affected by the heterogeneity. In order to estimate $\dfrac{\partial E_y}{\partial y}$ just outside the centre of the cylinder base, a 2nd degree polynomial was fitted to the electric field data in the homogeneous sphere (dashed curve in fig. 2) and an exponential curve was fitted to the difference in the electric field introduced by the inclusion. The sum of the two fitted curves was then differentiated to obtain the slope of the solid curve in fig. 2. The electric field distribution was calculated using a commercial finite element package (Comsol 3.2b with the

electromagnetics module, http://www.comsol.com/) and a frequency of 5 kHz was chosen for the time-harmonic analysis.

In order to assess the effect of the electric field discontinuity on the membrane potential of a myelinated axon, a model of the axon was implemented in which the axon is described as a sequence of compartments [14]. For myelinated sections, the membrane is described by a passive model consisting of a parallel RC circuit [15]. The membrane in each node of Ranvier is described by an active non-linear model based on data from the rabbit's myelinated axon [16]. In the first and last points of the discretized axon, sealed end boundary conditions were implemented [14]. The resulting set of equations was solved using the Picard iteration [17].

The electric field along the discretized axon was calculated using a model consisting of the Magstim 70 mm double coil placed over a heterogeneous volume conductor. The left half of the hexahedron had an electrical conductivity of 0.143 S/m, the right half had an electrical conductivity of 0.333 S/m [12], simulating a white matter–grey matter interface. Field calculations were performed using Comsol, as explained above. Two hundred electric field values, equally spaced along the axon, were exported to a file, for interpolation. The monophasic stimulus waveform used was very similar to the pulse generated by the Magstim 200 stimulator with the 70 mm double round coil.

III. RESULTS

For the homogeneous sphere, the electric field strength is greatest under the centre of the coil where it reaches 88.1 V/μs for a current rate of change of 67 A/μs, 15 mm below the scalp. The corresponding value of λE is 176 mV.

An example of the orientational dependence of the electric field's directional derivative is shown in fig. 1. This plot corresponds to one of the two grid points where the
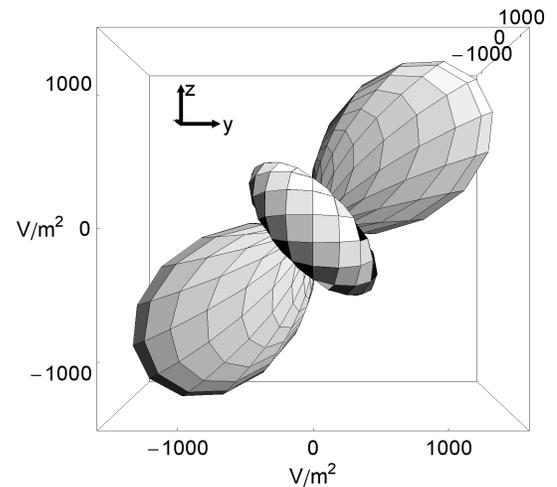

Fig. 1. Polar plot showing the magnitude of the directional derivative of the electric field as a function of angle, at the second grid point behind the coil centre. The top right lobe points approximately toward the centre of the coil.

directional derivative has its largest value, and is located 2 cm behind the coil centre, measured on the surface of the 77 mm radius sphere. The most negative value of the directional derivative occurs in the yz plane, along a direction 222° anticlockwise from the y-axis (lower left lobe in fig. 1). It amounts to -1896 V/m^2, which corresponds to a value of 7.6 mV for the activation function. The ratio of the activating function to the λE term is 4.3 %, and is independent of the rate of change of the current.

The plot in fig. 2 shows the variation of the component of the electric field parallel to the cylinder axis, E_y, as a function of position along that axis, both for a homogeneous sphere (dashed curve) and with the cylindrical inclusion (solid curve). The other components of the electric field are negligible. At the boundary, outside the inclusion, the values for λE_y and $\lambda^2 \dfrac{\partial E_y}{\partial y}$ are 199 mV and 24.2 mV, respectively. The ratio of these two terms is 12.2 %.
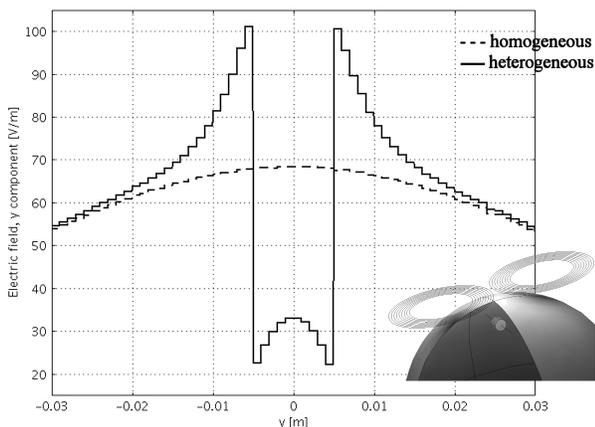

Fig. 2. Plot of the component of the electric field parallel to the cylinder axis, E_y, as a function of position along that axis for a homogeneous sphere (dashed curve) and a heterogeneous sphere (solid curve). Inset: position of high conductivity cylindrical inclusion, showing the segment of the cylinder axis along which data is plotted, 30 mm below the plane of the coil.

The axial component of the induced electric field along a straight axon that crosses at right angles an interface between two tissues with different conductivities is shown in fig. 3. The effect of this electric field distribution on the transmembrane potential is shown in fig. 4. Action potentials are generated at the electric field discontinuity and at the axon end that undergoes depolarization (right end), but not at the axon end that undergoes hyperpolarization (left end). With time the action potentials propagate away from the point of origin. As they collide, on the right half of the axon, propagation ceases due to the refractory state in which the portion of the membrane ahead has been left. The contours in the rising edge of the action potential are so close together that they appear as an almost solid black strip. The value of $\lambda \Delta E_y / 2$ is 79.5 mV, the value of λE_y at the depolarized axon end is 104.8 mV.
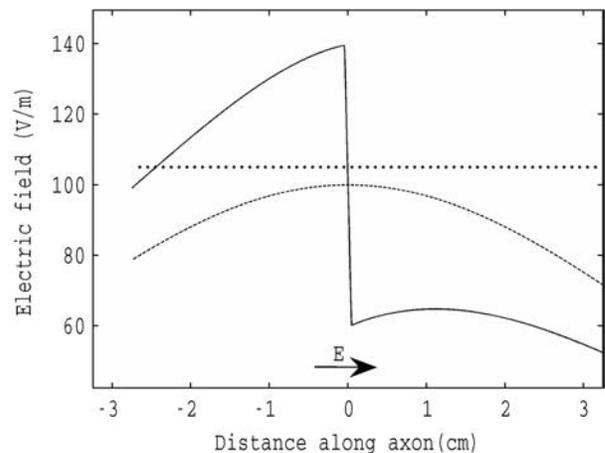

Fig. 3. Plot of the axial component of the electric field along a straight axon as it passes at right angles through an interface between two tissues with different conductivity values (solid curve) and for a homogeneous medium (dashed curve). The straight line shows the positions of the nodes of Ranvier on a 6 cm long axon.
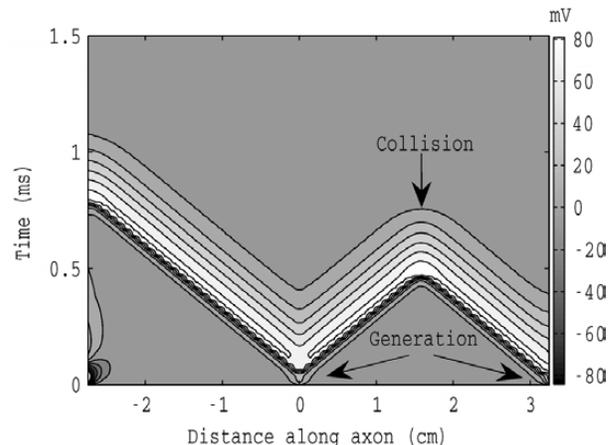

Fig. 4. Contour plot of the membrane potential, V', showing the generation and propagation of action potentials. An action potential is initiated at the middle of the axon by the electric field discontinuity and at the right end of the axon by the electric field. The left end of the axon is hyperpolarized at t=0.

IV. DISCUSSION

The calculations of the electric field and the electric field gradient induced in a homogeneous sphere show that the electric field and its directional derivative have their largest amplitudes at different locations and along different directions. Even when these differences are taken into account, the activation function has a considerably smaller maximum value than λE. Figure 1 shows the highly anisotropic nature of the directional derivative, whose angular dependence is far from intuitive. In this situation, the gradient component that is usually considered is 2.5 times smaller than the maximum directional derivative. Thus, in peripheral nerve stimulation or other cases where the electric field gradient may be the principal stimulation mechanism, calculations such as those presented here may be useful to optimize the experimental protocol.

The main conclusions to be drawn from the results obtained with the heterogeneous model is that internal

boundaries introduce strong local gradients compared to the homogeneous model and that the direction of the local gradient is also determined by the orientation of the interface, not only by the coil's configuration. Even so, the ratio of the maximum values of the activation function and λE remains small. Again, these considerations may be relevant in situations where the electric field gradient is the main stimulation mechanism.

The last set of calculations presented here confirms that an abrupt change in tissue conductivity can give rise to an action potential in a myelinated axon, even when the difference in electrical conductivities is modest and the boundary is positioned between two nodes of Ranvier. In the case shown, the stimulation threshold is lower at the right axon end than at the discontinuity because $\lambda \Delta E_y / 2$ is smaller than λE_y at that termination.

A comparison of the maximum values obtained for λE_x, $\lambda^2 \dfrac{\partial E_x}{\partial x}$ and $\lambda \Delta E_x / 2$ in the three conditions studied in this paper shows that the electric field term is the largest in all cases, indicating that the lowest threshold mechanism is likely to occur when axons end or bend in regions where the electric field has a strong component in the direction of the axon. When the axon's resistance to ionic flow along the direction of the applied electric field does not change sharply, the lowest threshold mechanism is the existence of an abrupt change in tissue conductivity along the path of the axon in the presence of a high electric field component perpendicular to the boundary. The electric field gradient term was always the smallest one but it can be significantly enhanced by tissue heterogeneity.

Variations in electrical conductivity will similarly affect the distribution of the electric field produced in electrical stimulation. Such effects may play an important role in transcranial direct current stimulation (tDCS).

This realization of tissue heterogeneity as a source of neural excitation has potentially important consequences to transcranial magnetic stimulation (TMS) in particular, and to understanding the interaction of electric fields and tissue, in general. First, differences in electrical conductivity among grey matter, white matter, and cerebrospinal fluid alone could result in depolarization or hyperpolarization of excitable tissues at or near interfaces between them. This mechanism of activation thus could provide a possible explanation for the observation of "far field" stimulation of brain and other tissues. So, for example, this mechanism could be implicated in explaining the recent finding that Echo Planar MRI of brain can effect a mood change in normal subjects [18]. Such an apparent TMS-like effect from switched magnetic field gradients is not expected using a conventional "activating function".

Secondly, this new mechanism should be investigated in the context of assessing possible health effects of high-tension transmission lines upon tissue. Charge may build up transiently across membrane boundaries or structures that are oriented perpendicular to the local induced electric field, leading to transport of charged molecules. This new mechanism suggests how biological effects may be caused by far-field electromagnetic sources.

REFERENCES

[1] P. J. Basser and B. J. Roth, "Stimulation of a myelinated nerve axon by electromagnetic induction," *Med Biol Eng Comput*, vol. 29, pp. 261-8, 1991.

[2] B. J. Roth and P. J. Basser, "A model of the stimulation of a nerve fiber by electromagnetic induction," *IEEE Trans Biomed Eng*, vol. 37, pp. 588-97., 1990.

[3] B. J. Roth, "Mechanisms for electrical stimulation of excitable tissue," *Crit Rev Biomed Eng*, vol. 22, pp. 253-305, 1994.

[4] J. P. Reilly, "Principles of nerve and heart excitation by time-varying magnetic fields," *Ann N Y Acad Sci*, vol. 649, pp. 96-117, 1992.

[5] P. S. Tofts, "The distribution of induced currents in magnetic stimulation of the nervous system," *Phys Med Biol*, vol. 35, pp. 1119-28., 1990.

[6] B. J. Roth, J. M. Saypol, M. Hallett, and L. G. Cohen, "A theoretical calculation of the electric field induced in the cortex during magnetic stimulation," *Electroencephalogr Clin Neurophysiol*, vol. 81, pp. 47-56, 1991.

[7] P. J. Maccabee, V. E. Amassian, L. P. Eberle, A. P. Rudell, R. Q. Cracco, K. S. Lai, and M. Somasundarum, "Measurement of the electric field induced into inhomogeneous volume conductors by magnetic coils: application to human spinal neurogeometry," *Electroencephalogr Clin Neurophysiol*, vol. 81, pp. 224-37, 1991.

[8] R. Liu and S. Ueno, "Calculating the activation function of nerve excitation in inhomogeneous volume conductor during magnetic stimulation using the finite element method," *IEEE Trans Magn*, vol. 36, pp. 1796-9, 2000.

[9] P. C. Miranda, M. Hallett, and P. J. Basser, "The electric field induced in the brain by magnetic stimulation: a 3-D finite-element analysis of the effect of tissue heterogeneity and anisotropy," *IEEE Trans Biomed Eng*, vol. 50, pp. 1074-85, 2003.

[10] A. Thielscher and T. Kammer, "Linking physics with physiology in TMS: a sphere field model to determine the cortical stimulation site in TMS.," *Neuroimage*, vol. 17, pp. 1117-30, 2002.

[11] H. Eaton, "Electric field induced in a spherical volume conductor from arbitrary coils: application to magnetic stimulation and MEG," *Med Biol Eng Comput*, vol. 30, pp. 433-40, 1992.

[12] J. Haueisen, C. Ramon, M. Eiselt, H. Brauer, and H. Nowak, "Influence of tissue resistivities on neuromagnetic fields and electric potentials studied with a finite element model of the head," *IEEE Trans Biomed Eng*, vol. 44, pp. 727-35, 1997.

[13] S. B. Baumann, D. R. Wozny, S. K. Kelly, and F. M. Meno, "The electrical conductivity of human cerebrospinal fluid at body temperature," *IEEE Trans Biomed Eng*, vol. 44, pp. 220-3, 1997.

[14] S. S. Nagarajan, D. M. Durand, and E. N. Warman, "Effects of induced electric fields on finite neuronal structures: a simulation study," *IEEE Trans Biomed Eng*, vol. 40, pp. 1175-88, 1993.

[15] P. J. Basser, "Scaling laws for myelinated axons derived from an electrotonic core-conductor model," *J Integr Neurosci*, vol. 3, pp. 227-44, 2004.

[16] E. N. Warman, W. M. Grill, and D. Durand, "Modeling the effects of electric fields on nerve fibers: determination of excitation thresholds," *IEEE Trans Biomed Eng*, vol. 39, pp. 1244-54, 1992.

[17] M. V. Mascagni and A. S. Sherman, "Numerical methods for neuronal modeling," in *Methods in Neuronal Modeling: from Ions to Networks, Computational neuroscience*, C. Koch and I. Segev, Eds., 2nd ed. Cambridge, Mass.: MIT Press, 1998, pp. xiii, 671.

[18] M. Rohan, A. Parow, A. L. Stoll, C. Demopulos, S. Friedman, S. Dager, J. Hennen, B. M. Cohen, and P. F. Renshaw, "Low-field magnetic stimulation in bipolar depression using an MRI-based stimulator," *The American journal of psychiatry*, vol. 161, pp. 93-8, 2004.